JOURNAL OF CATALYSIS **161,** 132–142 (1996)
ARTICLE NO. 0170

Selectivity to Olefins of Fe/SiO_2–MgO Catalysts in the Fischer–Tropsch Reaction

N. G. Gallegos, A. M. Alvarez, M. V. Cagnoli, J. F. Bengoa, S. G. Marchetti, R. C. Mercader, and A. A. Yeramian

Centro de Investigación y Desarrollo en Procesos Catalíticos (CINDECA, CONICET), Facultad de Ciencias Exactas (UNLP), Facultad de Ingeniería (UNLP), and Comisión de Investigaciones Científicas de la Pcia.de Bs.As. (CIC), Calle 47, 257, La Plata 1900, Argentina

Received May 31, 1995; revised January 4, 1996; accepted February 5, 1996

SiO_2 covered with MgO has been used as support of iron catalysts in the Fischer–Tropsch reaction. Catalysts of 5% (w/w) iron concentration and 2, 4, and 8% (w/w) of MgO on SiO_2 were prepared. Selective chemisorption of CO, volumetric oxidation, and Mössbauer spectroscopy were used to characterize the type of iron species and the metallic crystal sizes. MgO covers the SiO_2 surface and modifies the metallic crystal size. The activity to total hydrocarbons increases with the amount of MgO added. An optimal concentration of about 4% (w/w) was found to have the highest selectivity to olefins.

INTRODUCTION

The use of supported metallic catalysts in the Fischer–Tropsch synthesis has been extensively studied in the past years (1–16). Nevertheless, a catalyst selective to some interesting products like light olefins and with an acceptable activity is still an unresolved problem.

Previously (17), we have been able to corroborate that a basic support like MgO has an improved selectivity to light olefins compared to Fe catalysts supported on typical materials like SiO_2 and Al_2O_3 (17, 18).

However, MgO alone presents drawbacks as a support. Its low surface area leads to a poor dispersion of the active phase, and the very easy way in which it is carbonated or hydroxilated, once in contact with air, leads to changes in its main catalytic features.

With the intention of keeping the good selectivity to olefins, while increasing the surface exposed to the reactants and improving the stability of the solid, iron catalysts supported on silica covered with different amounts of MgO have been prepared. In this paper we report the study of the activity, selectivity and basicity, and particle size effects of these catalysts.

METHODS

Preparation of the Catalysts

Five precursors of the catalysts of approximately 5% (w/w) of Fe were prepared: Fe supported on SiO_2 (p-0), Fe supported on SiO_2 onto which 2, 4, and 8% (w/w) of MgO were added (p-2, p-4, and p-8) and, as a test sample, a precursor of Fe supported on MgO (p-t).

The p-0 was made by dry impregnation of Kieselgel-100 (Merck) silica gel, with 400 m^2/g specific area, 1 cm^3/g pore volume and 0.06–0.20 mm particle size. An impregnating solution of pH 0.5 of $Fe(NO_3)_3 \cdot 9H_2O$ with a high enough concentration to yield a catalyst of ca. 5% (w/w) was used. The precursor was air dried at room temperature for 20 days and then calcinated in air at 698 ± 5 K for 8 h.

The precursors p-2, p-4, and p-8 were prepared in two steps: (a) dry impregnation of silica gel with a solution of $Mg(NO_3)_2$ and air calcination at 698 ± 5 K during 8 h, (b) dry impegnation of the resulting SiO_2–MgO support with $Fe(NO_3)_3 \cdot 9H_2O$. Further drying and calcination were carried out in identical conditions as for p-0. All samples were introduced into the oven once its temperature had reached 698 ± 5 K.

The precursor of Fe/MgO was prepared by a technique recommended by Boudart *et al.* (19). A suspension of magnesium hydroxycarbonate (MHC, Carlo Erba) in demineralized water was mechanically stirred and heated at 337 K. A solution of $Fe(NO_3)_3 \cdot 9H_2O$, prepared with a concentration calculated to get a catalyst of ca. 5% (w/w) of iron, was added to that suspension. The slurry was kept at 337 K during 30 min with stirring. Once this period was over, the slurry was centrifuged and the solid washed with demineralized water. Afterward, it was calcinated in air at 698 ± 5 K for 8 h (p-t).

All precursors were reduced in H_2 stream according to a program reported in Ref. (18). Catalysts c-0, c-2, c-4, c-8, and c-t are the final products of the reduction.

Characterization Techniques

CO chemisorption. Measurements were made on the catalysts in a conventional static volumetric equipment with grease-free vacuum valves using CO as titration reagent as described in (18).

Volumetric oxidation. Volumetric oxidation experiments were performed in the adsorption equipment

0021-9517/96 $18.00

described above. These experiments were based on the fact that, above 620 K in O_2, all the iron species present in the catalyst in oxidation states lower than Fe^{3+} oxidize to Fe_2O_3 (19). Once reduced, the samples were evacuated and oxidized with an appropriate amount of O_2 at 620 K. The experiment was completed when oxygen pressure variation no longer occurred. The uptake of O_2 was thus determined.

Mössbauer spectroscopy. The Mössbauer spectra were obtained in transmission geometry, with a 512-channel constant acceleration spectrometer. A source of ^{57}Co in Rh matrix of nominally 100 mCi was used. Velocity calibration was performed against a 6-μm-thick α-Fe foil. All isomer shifts (IS) mentioned in this paper are referred to this standard. The temperature between 17 and 298 K was varied using a Displex DE-202 closed cycle cryogenic system.

The Mössbauer spectra of the catalysts were obtained *in situ* using a cell specially built for this purpose to be used inside the cryogen from 25 to 298 K (20).

All spectra were fitted with a program including hyperfine parameters distributions (21) generated by the different particle sizes and/or different crystallographic sites of the iron phases present. The spectra were folded to minimize geometric effects.

Activity and selectivity measurements. Measurements of activity and selectivity were carried out during 48 h using a fixed bed reactor at 543 K, 1013 N/m^2 and $H_2:CO$ ratio of 3:1. The data shown in this paper correspond to the pseudo-steady state (30 h stream time for all catalysts). The experimental equipment has been described in a previous work (18).

The products were analyzed in a Konik Chromatograph having a flame ionization detector using a GS-Alumina PLOT (J&W Scientific) column.

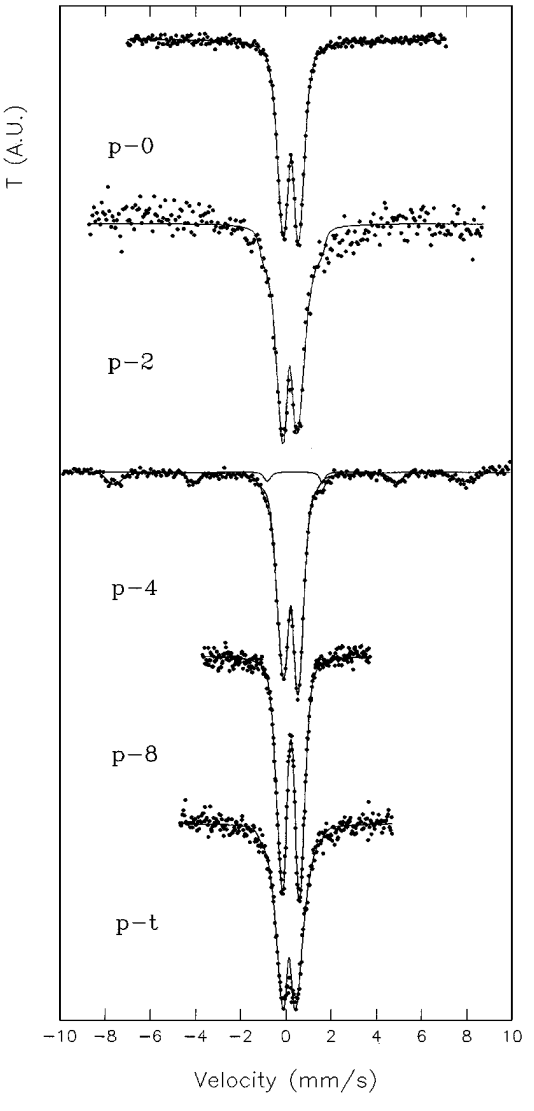

FIG. 1. Mössbauer spectra of the precursors at 298 K.

RESULTS AND DISCUSSION

Precursor characterization. Figures 1 and 2 show the Mössbauer spectra corresponding to precursors obtained at 298 and 17 K, respectively. Only the central part of spectra p-8 and p-t are displayed because no magnetic signal is present at higher velocities (and therefore a narrower velocity range was used). The same patterns were observed for intermediate temperatures and are not significant for the discussion.

In supported samples the crystallite size distribution may produce a considerable variation in the local surroundings of the Mössbauer atoms and the IS, H, and ΔQ for the individual atoms may therefore vary considerably (22). Such variations often lead to unequal line broadening in the spectra. As a first-order approximation a linear correlation between these two hyperfine parameters can be assumed (21, 22). To take account of these hyperfine fields distributions the IS was assumed to be linearly correlated with the magnetic hyperfine field (H) and/or quadrupole splitting (ΔQ) for all fittings.

The most likely values of the hyperfine parameters are characteristic of Fe^{3+} species (Figs. 3 and 4 and Table 1) for all spectra. These parameters can be assigned to three different Fe^{3+} species: very small size superparamagnetic microcrystals of α-Fe_2O_3 (19, 23, 24), amorphous Fe_2O_3 (25), and Fe^{3+}, either exchanged at the surface of the support, or forming a solid solution with the support, or being part of a surface or bulk compound (26, 27).

p-4 is the only precursor which shows a magnetic signal even at room temperature (in addition to the superparamagnetic doublet). At 17 K its fraction increases and the hyperfine magnetic field is 5% lower than that of bulk α-Fe_2O_3 at the same temperature.

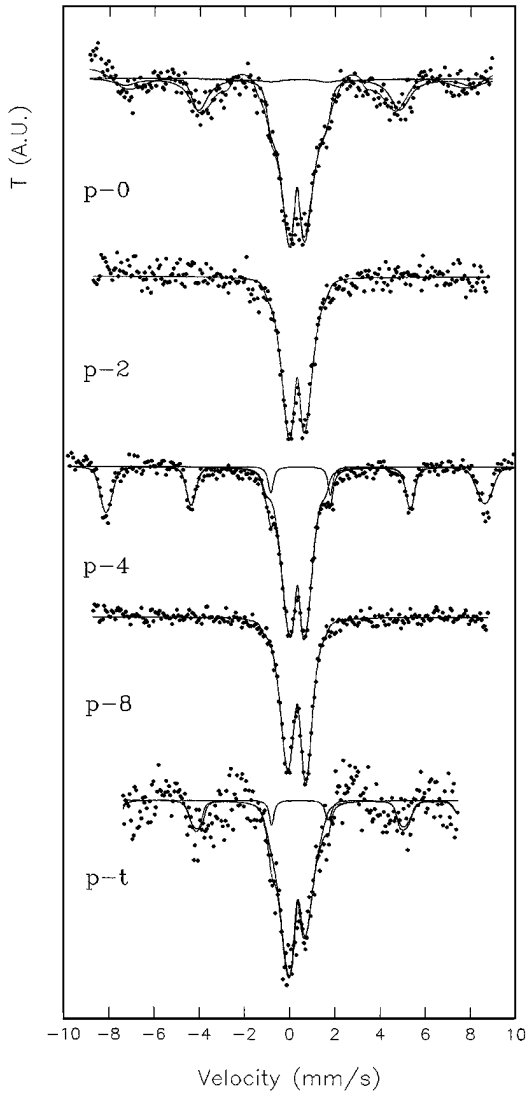

FIG. 2. Mössbauer spectra of the precursors at 17 K.

The collective magnetic excitation model predicts that, because of thermal fluctuations, the observed hyperfine magnetic field decreases to an amount determined by (28):

$$H_{OBS} = H_0\left[1 - \frac{k_B T}{2KV}\right], \qquad [1]$$

where

H_0 is the magnetic hyperfine field of the bulk α-Fe_2O_3 (540 kG at 17 K);
k_B, Boltzmann constant;
K, magnetic anisotropy energy constant;
V, particle volume;
T, temperature.

A K value of $(0.5 \pm 0.2)\ 10^5$ J m^{-3}, has been estimated for α-Fe_2O_3 particles of about 120 Å (1 Å $= 10^{-10}$ m) (28). Using this estimate from Eq. [1] an average particle size of approximately 50 Å can be calculated. Due to the dependence of K on V, this value must be considered only as a rough estimate.

The superparamagnetic (Sp) fraction can be due to α-Fe_2O_3 microcrystals with a blocking temperature lower than 17 K or to Fe^{3+} migrated into the support, as was earlier mentioned.

p-0 and p-t show magnetic splitting at 17 K, but, in both cases H_{OBS} is too low to be explained by the collective magnetic excitation model. Probably this signal is denoting the existence of amorphous Fe_2O_3 since its parameters are close to those of this oxide prepared by sputtering (25). The particle size of these compounds would be around 48 Å, obtained from a comparison with those of Bødker *et al.* (25). The same consideration as for p-4 is applied to the sp signal.

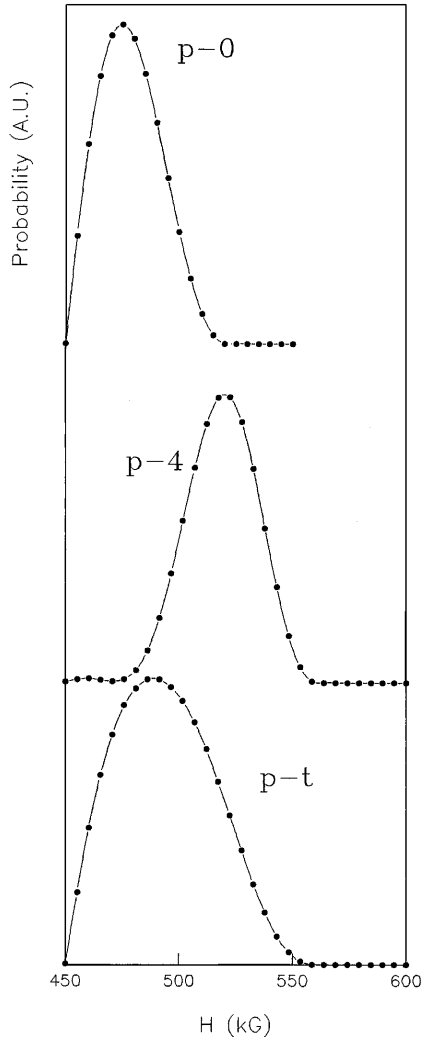

FIG. 3. Hyperfine field distribution of magnetic Fe^{3+} of the precursors at 17 K.

TABLE 1

Most Likely Values of Mössbauer Parameters for Different Precursors after Distribution Fittings Described in the Text

Species	Parameters[a]	p-0	p-2	p-4	p-8	p-t
			17 K			
Superparamagnetic Fe^{3+}	IS (mm/s)	0.43 ± 0.02	0.43 ± 0.01	0.44 ± 0.01	0.43 ± 0.01	0.45 ± 0.03
	ΔQ (mm/s)	0.79 ± 0.03	0.72 ± 0.01	0.74 ± 0.01	0.82 ± 0.01	0.62 ± 0.04
	%	71 ± 9	100 ± 8	67 ± 3	100 ± 3	70 ± 12
Magnetic Fe^{3+}	IS (mm/s)	0.50 ± 0.04	—	0.47 ± 0.01	—	0.35 ± 0.06
	ΔQ (mm/s)	-0.03 ± 0.03	—	-0.23 ± 0.01	—	-0.43 ± 0.05
	H (kG)	477 ± 3	—	519 ± 1	—	489 ± 5
	%	29 ± 9	—	33 ± 3	—	30 ± 6
			298 K			
Superparamagnetic Fe^{3+}	IS (mm/s)	0.35 ± 0.01	0.31 ± 0.01	0.33 ± 0.01	0.33 ± 0.01	0.27 ± 0.01
	ΔQ (mm/s)	0.70 ± 0.01	0.71 ± 0.01	0.67 ± 0.01	0.78 ± 0.01	0.65 ± 0.01
	%	100 ± 2	100 ± 8	85 ± 3	100 ± 2	100 ± 2
Magnetic Fe^{3+}	IS (mm/s)	—	—	0.40 ± 0.03	—	—
	ΔQ (mm/s)	—	—	-0.24 ± 0.03	—	—
	H (kG)	—	—	480 ± 2	—	—
	%	—	—	15 ± 2	—	—

[a] All isomer shifts are referred to α-Fe.

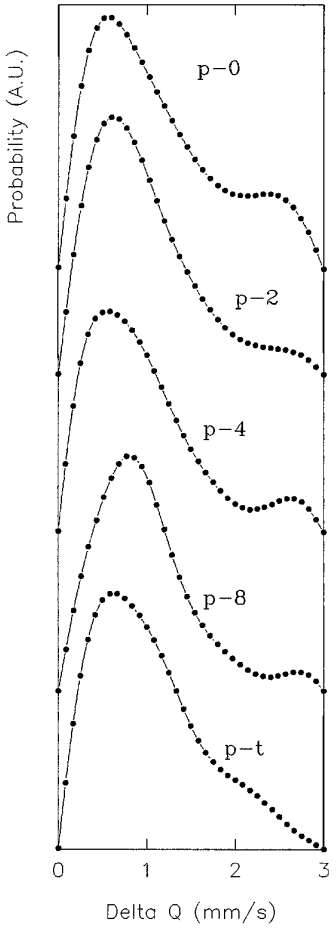

FIG. 4. Quadrupole splitting distribution of superparamagnetic Fe^{3+} of the precursors at 17 K.

Precursors p-2 and p-8 show at both temperatures doublets assignable to very small size superparamagnetic Fe_2O_3 microcrystals with blocking temperature lower than 17 K and/or Fe^{3+} migrated into the support. In the first case the average diameter would be lower than 50 Å.

Characterization of the reduced catalysts. The Mössbauer spectra of the *in situ* reduced catalysts at 298 and 25 K (Figs. 5 and 6) display a central part with many overlapped signals belonging to different iron species. According to the measured IS values Fe^0, Fe^{2+}, and Fe^{3+} can be present in all of them. Mössbauer spectra showing such a large overlapping in the central region make of doubtful validity the assignment based only on least-squares fitting of the spectra. This is true even if hyperfine field distributions are used. Based on reasons which will be described below, the fits were done in the following way: c-0, c-2, c-4, and c-8 catalysts show a singlet with IS = 0.0 and 0.16 mm/s at 298 and 25 K, respectively, that was assigned to Fe^0 (sp) (25, 26, 29, 30).

c-4 also displayed a magnetic signal with a hyperfine field of approximately 330 kG at 298 K that increased at 25 K. This signal was assigned to magnetic iron, Fe^0(m) (23). The magnetic signal intensity increased while the superparamagnetic one decreased when the temperature was lowered from 298 to 25 K. For c-t the magnetically split signal was the only one assignable to Fe^0.

The rest of the signals were fitted with two doublets. One of them showed parameters assignable to Fe^{2+} (19, 31) and the other one to Fe^{3+}. The possibility of the migration of Fe^{3+} into the support of the precursor was confirmed by two facts: (a) the presence of Fe^{3+} in all reduced catalysts,

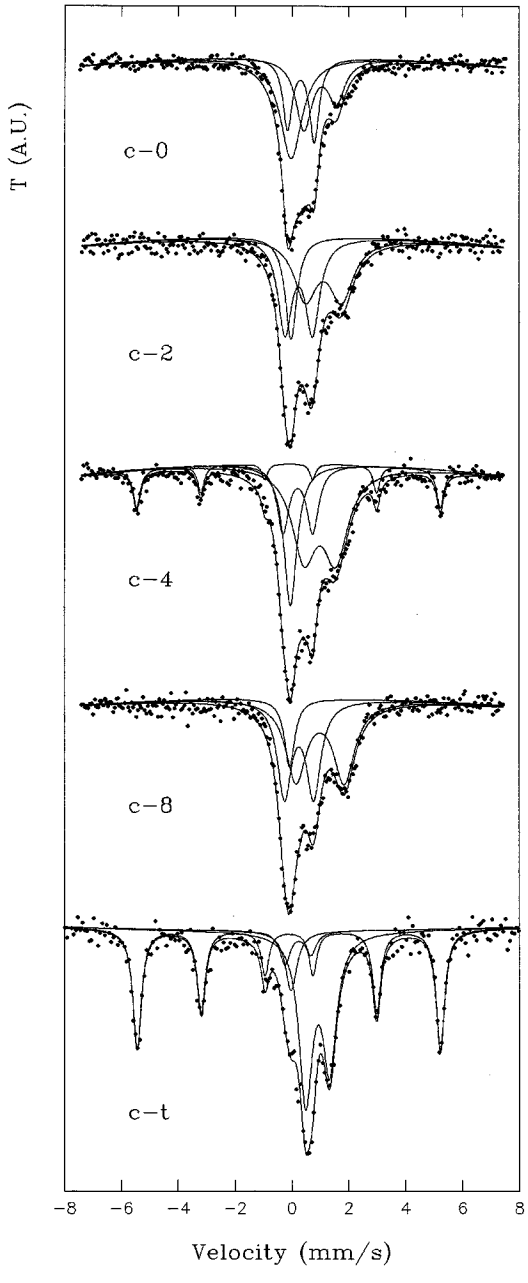

FIG. 5. Mössbauer spectra of the reduced catalysts at 298 K.

(b) the fact that Fe^{3+} signal does not appear magnetically split even at 25 K. Table 2 shows the most likely hyperfine parameters for all catalysts.

To check that the presence of Fe^{3+} was not due to a malfunction of the *in situ* Mössbauer cell, its capacity to keep the reducing atmosphere was verified carrying out the following test:

—A Mössbauer spectrum was obtained with c-0 in the cell.

—Afterward, the catalyst was exposed to air and a new Mössbauer spectrum was taken at room temperature.

A comparison of these spectra shows dissimilarities that denote that they belong to different species originated when the sample was reoxidized (Fig. 7). More details of this experiment and the cell design will be published elsewhere (20).

It is noteworthy that fittings with lorentzian line shapes, without hyperfine parameters distributions, lead to very high IS values for Fe^0(sp), a lack of second-order Doppler shift for all species, and unrealistic asymmetries of the intensities of the quadrupole doublets components for Fe^{2+} and Fe^{3+}.

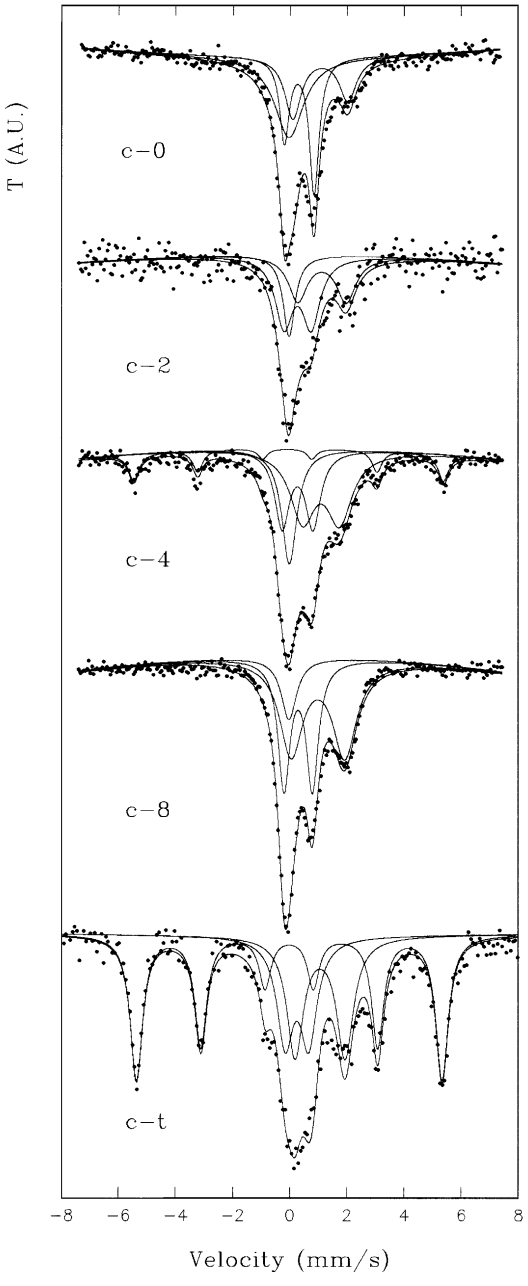

FIG. 6. Mössbauer spectra of the reduced catalysts at 25 K.

TABLE 2

Most Likely Values of Mössbauer Parameters for Reduced Catalysts after Distribution Fittings Described in the Text

Species	Parameters[a]	c-0	c-2	c-4	c-8	c-t
			25 K			
Superparamagnetic Fe^0	IS (mm/s)	0.16 ± 0.08	0.16 ± 0.18	0.17 ± 0.06	0.16 ± 0.08	—
Magnetic Fe^0	IS (mm/s)	—	—	0.04 ± 0.01	—	0.10 ± 0.01
	ΔQ (mm/s)	—	—	0.05 ± 0.01	—	0.00 ± 0.01
	H (kG)	—	—	337 ± 1	—	333 ± 1
Fe^{2+}	IS (mm/s)	1.17 ± 0.09	1.21 ± 0.10	1.05 ± 0.15	1.09 ± 0.20	1.18 ± 0.02
	ΔQ (mm/s)	1.95 ± 0.18	1.79 ± 0.22	1.69 ± 0.30	1.88 ± 0.40	1.78 ± 0.05
Fe^{3+}	IS (mm/s)	0.46 ± 0.10	0.40 ± 0.15	0.42 ± 0.03	0.40 ± 0.02	0.40 ± 0.05
	ΔQ (mm/s)	0.97 ± 0.20	0.96 ± 0.30	0.95 ± 0.12	0.97 ± 0.05	0.71 ± 0.11
			298 K			
Superparamagnetic Fe^0	IS (mm/s)	0.08 ± 0.09	0.01 ± 0.04	0.02 ± 0.03	0.09 ± 0.08	—
Magnetic Fe^0	IS (mm/s)	—	—	0.01 ± 0.01	—	0.01 ± 0.01
	ΔQ (mm/s)	—	—	-0.02 ± 0.01	—	-0.01 ± 0.01
	H (kG)	—	—	331 ± 1	—	330 ± 1
Fe^{2+}	IS (mm/s)	0.89 ± 0.05	1.00 ± 0.10	0.86 ± 0.08	1.01 ± 0.02	0.97 ± 0.10
	ΔQ (mm/s)	1.17 ± 0.12	1.29 ± 0.18	1.36 ± 0.15	1.63 ± 0.04	1.51 ± 0.19
Fe^{3+}	IS (mm/s)	0.37 ± 0.14	0.35 ± 0.03	0.33 ± 0.02	0.36 ± 0.03	0.32 ± 0.02
	ΔQ (mm/s)	0.80 ± 0.31	1.03 ± 0.09	0.87 ± 0.08	0.91 ± 0.06	0.77 ± 0.05

[a] All isomer shifts are referred to α-Fe.

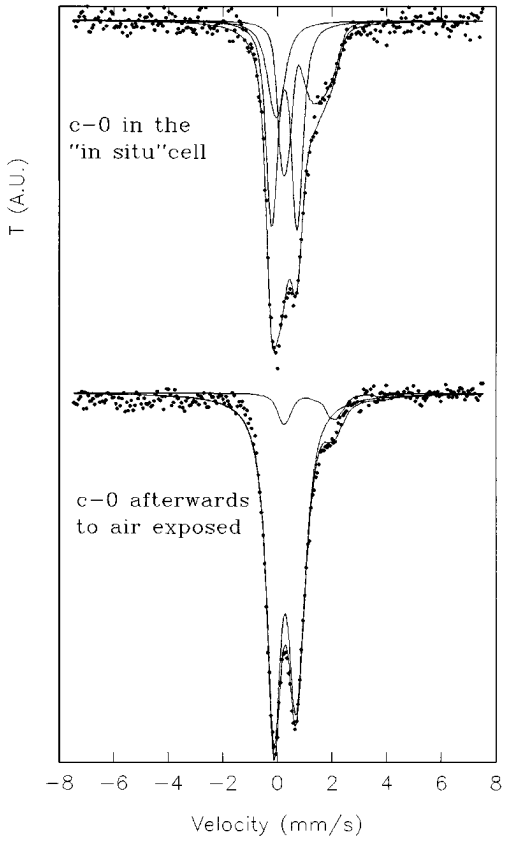

FIG. 7. Mössbauer spectra of c-0 catalyst in the *in situ* cell and after being exposed to air at 298 K.

Table 3, shows the results of oxygen uptake, obtained after the volumetric oxidation of the catalysts. There is a good agreement between the experimental oxygen uptake for the complete reoxidation of the reduced catalysts and the consumption of oxygen calculated from the percentage of each species obtained from the Mössbauer spectra at 25 K assuming equal *f*-factors for all iron species.

Equal recoiless factors were used based in the following considerations. If the Debye model for the different iron species is assumed to describe the lattice vibrations, although the actual Debye temperatures (θ_D) for each species are not known, at 25 K a variation of the θ_D between species as high as 300 K (from 200 to 500 K) would produce only a decrease of about 6% in their *f*-factors (32).

Other choices for the assignments of the iron species different from that of Table 3 lead to unacceptable differences between both techniques. In brief, if it is considered that in c-0 catalyst only Fe^{2+} and Fe^{3+} are present (Fig. 8 and Table 4) the fit quality is poorer (χ^2 changes from 1.1 to 1.5 at 298 K and from 1.4 to 2.6 at 25 K) and the O_2 uptake calculated (116 μmol O_2/g catalyst) is significantly smaller than the volumetric oxidation value (392 μmol O_2/g catalyst). This is further evidence confirming the Fe^0 existence in c-0 catalyst. The same results were found in the rest of the catalysts. This cross-checking of volumetric oxidation results with the complex Mössbauer spectra of these catalysts is the only reliable method that should be used in spectra of such complexity if one has not the capability to take *in situ* spectra of samples with an external magnetic field.

TABLE 3

Characterization Data of the Catalysts

	Species (%)			n^a_{CO}	n^b_{CO}	d_{VA}	O_2 uptake (μmol/g_{cat})	
	Fe^0_t	Fe^{2+}	Fe^{3+}	(μmol/g_{cat})	(μmol/g_{supp})	(Å)	Vol. oxidation	Mössbauer
c-0	33 ± 3	31 ± 2	36 ± 2	37 ± 2	0	35	392 ± 20	334 ± 40
c-2	18 ± 7	32 ± 5	50 ± 9	50 ± 3	26 ± 1	35	298 ± 15	271 ± 73
c-4	36 ± 14	39 ± 7	25 ± 11	33 ± 2	17 ± 1	66	274 ± 14	289 ± 68
c-8	9 ± 1	56 ± 3	35 ± 2	41 ± 2	23 ± 1	21	221 ± 11	230 ± 12
c-t	46 ± 3	33 ± 1	21 ± 1	14 ± 1	6 ± 1	179	369 ± 18	352 ± 21

Note: Fe^0_t, total Fe^0; n^a_{CO}, number of micromoles chemisorbed per gram of catalyst; n^b_{CO}, number of micromoles chemisorbed per gram of support; d_{VA}, average volumetric–superficial diameter; g_{cat}, grame of catalyst; g_{supp}, grame of support.

Although the five catalysts contain the same Fe species, their metallic crystal sizes are different. c-4 shows the existence of Fe^0(sp) and Fe^0(m) at room temperature. The first fraction corresponds to very small metallic crystals. c-0, c-2, and c-8 do not show the presence of Fe^0(m) even at temperatures as low as 25 K, while in c-t only Fe^0(m) is found at both temperatures. According to this, the following Fe particle size order is proposed:

$$\text{c-2} \approx \text{c-8} \approx \text{c-0} < \text{c-4} < \text{c-}t.$$

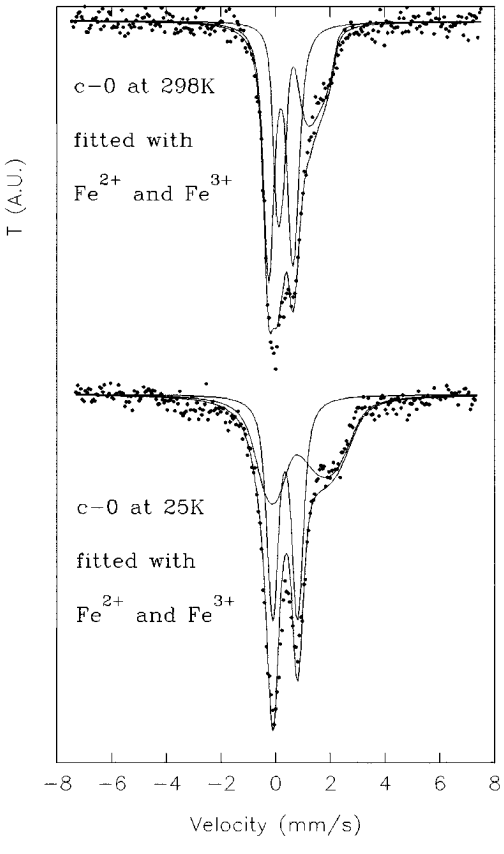

FIG. 8. Mössbauer spectra of c-0 catalyst fitted with Fe^{2+} and Fe^{3+} at 298 and 25 K.

No MgO signal could be detected by X-ray diffraction, indicating that it might be present as very small crystallites or as a layer on the silica. The last alternative seems to be more plausible since measurements of chemisorption of CO on the supports of c-2, c-4, and c-8 do not show significant differences for a MgO concentration that has increased four times from c-2 to c-8 (Table 3). This gives further support to the idea that the surface of silica is already totally covered with magnesia for c-2; that can be expected since a simple calculation based on the specific surface area of SiO_2 and the area covered by the MgO unit cell shows that 2% of magnesia is sufficient for completing a monolayer on the exposed SiO_2 surface. In addition, no lines belonging to other compounds that might have been originated by a possible reaction between MgO and SiO_2 were observed in the X-ray diffraction patterns carried out on all supports.

We describe next a tentative model to account for the influence of MgO on the catalyst:

- Catalyst c-2 undergoes a surface coating without important changes in the pore distribution of SiO_2 (maxima at 30, 40, 50, and 60 Å determined by adsorption–desorption of N_2 (Fig. 9)).
- The pore diameters smaller than 50 Å are partially filled in the catalyst c-4. The maximum at 60 Å is slightly displaced to 55 Å.
- For c-8 the filling of the pores continues. This process generates new micropores of smaller diameters (a zone

TABLE 4

Most Likely Values of Mössbauer Parameters for c-0 Fitted with Fe^{2+} and Fe^{3+}

Species	Parameters	298 K	25 K
Fe^{2+}	IS (mm/s)	0.75 ± 0.05	1.01 ± 0.02
	ΔQ (mm/s)	1.14 ± 0.02	2.03 ± 0.05
Fe^{3+}	IS (mm/s)	0.31 ± 0.04	0.46 ± 0.04
	ΔQ (mm/s)	0.83 ± 0.05	0.83 ± 0.05

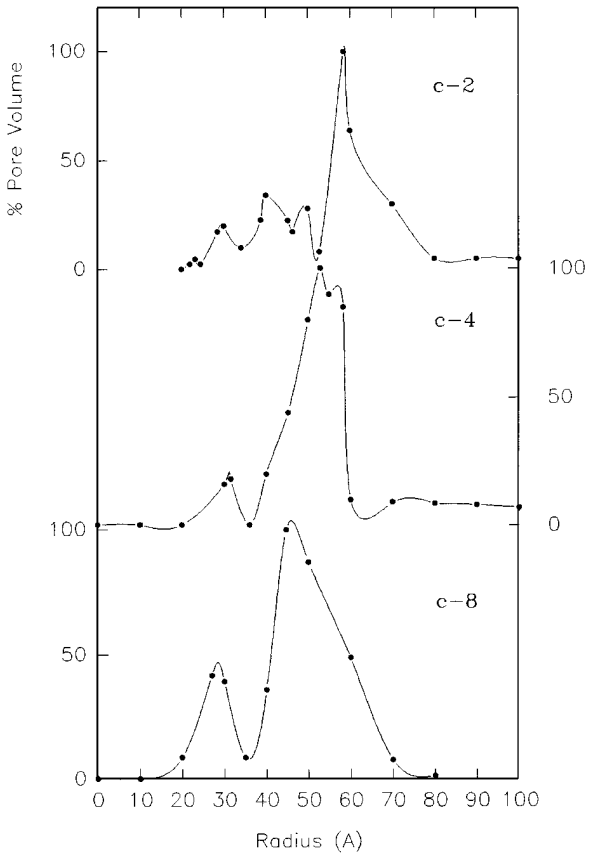

FIG. 9. Pore volume distribution in the SiO_2–MgO supports.

between 15 and 35 Å) and a new displacement of the diameters of the bigger pores (maximum at 45 Å).

This model, together with the iron crystal sizes deduced from the Mössbauer spectra, gives the following size sequence:

$$\text{c-8} < \text{c-2} < \text{c-4}.$$

Size determination cannot be done by direct means because the use of electron microscopy is not possible due to the high Fe^0 reoxidation capacity: other techniques must be used. CO chemisorption is a suitable technique for measuring the particle size and has been frequently used in many papers (5, 19, 33, 34). The D_{VA} (average surface volumetric diameter) of Fe^0, calculated from CO chemisorption measurements on reduced catalysts as in (18), are displayed in Table 3. These results are coincident with the sequence of particle sizes deduced earlier.

Activity and selectivity measurements. The products detected under reaction conditions, mentioned earlier, have been $CH_4(C_1)$, $C_2H_6(C_2)$, $C_3H_8(C_3)$, $C_4H_{10}(C_4)$, $C_2H_4(C_2^=)$, $C_3H_6(C_3^=)$, and $C_4H_8(C_4^=)$. No oxygenate compounds were found in any case. All catalysts produced a similar CO conversion (X) at pseudo-steady state (X(c-0) = 1.4%, X(c-2) = 0.9%, X(c-4) = 0.9%, X(c-8) = 1.6%, and X(c-t) = 1.4%). A decrease of about 16% in ethylene/ethane and propene/propane ratios when CO conversion increased from 1 to 2% was found by Amelse *et al.* (35) and Butt (36) for a 4.9% (w/w) Fe/SiO_2 catalyst. Moon *et al.* (37) have got an ethylene/ethane ratio constant in practice for a CO conversion varying between 1 and 2% when they studied the catalytic behavior of 9% (w/w) Fe/SiO_2 catalysts with different reduction degree. Rameswaran and Bartholomew (38) reported a constant olefins/paraffins ratio over a CO conversion range of 0.60–1.71% for a 4.5% (w/w) Fe/Al_2O_3 catalysts.

The selectivity variations found in this work are larger than 30% in a 0.9–1.6% CO conversion range. Consequently, its influence was not considered in the activity and the selectivity results reported here.

Figure 10 displays the turnover frequency for total hydrocarbon produced at 30 h. To calculate the turnover frequency one active site per atom of surface Fe^0 was considered. The number of Fe atoms at the surface was evaluated from the chemisorption experiments mentioned above (18). An increase of the turnover frequency with the amount of MgO on SiO_2 can be noticed.

According to the assigned crystal size, one should expect certain relation of activities (39). The results obtained indicate that the increase in basicity of the support produces an enhancement of the intrinsic activity of each metallic site. This effect predominates over that due to the crystal size. This is an indication that although the reaction is sensitive to the structure (39), the close contact of the iron with MgO modifies the activity sequence expected according to the metallic crystal sizes.

Figure 11 shows the olefin to paraffin ratio ($[C_2^= + C_3^= + C_4^=]/[C_1 + C_2 + C_3 + C_4]$) for the different catalysts. The ratio increases up to 0.66 for c-4 (similar to c-t) and drops to 0.18 for c-8.

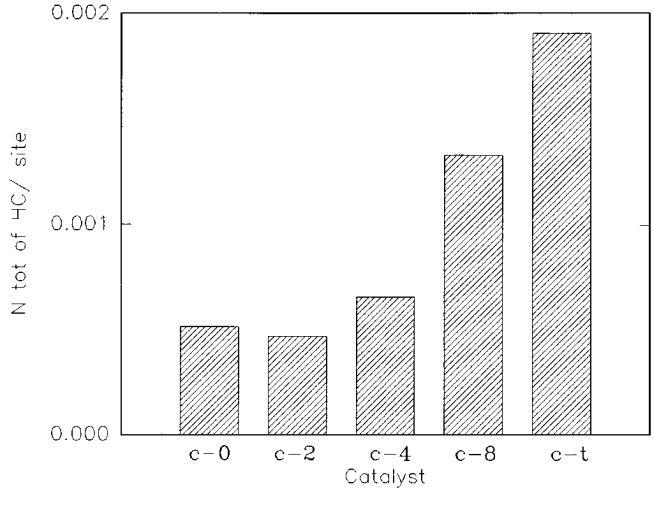

FIG. 10. Total turnover frequency of the catalysts at steady state.

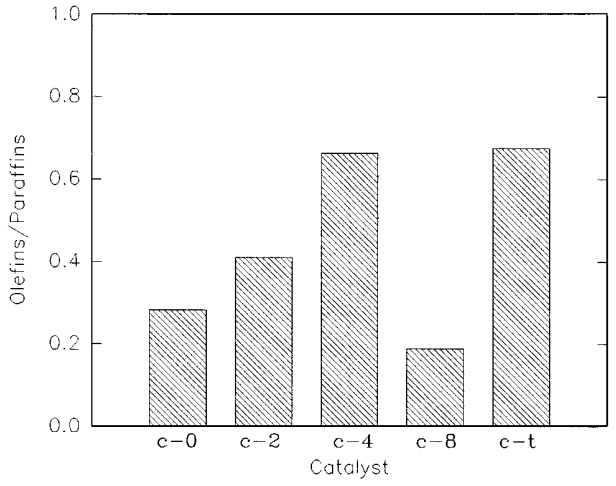

FIG. 11. Olefins/paraffins ratio of the catalysts at steady state.

This behavior could be explained considering the following scheme for the Fischer–Tropsch reaction mechanism (40):

$$(1)\qquad CO + 2S^* \rightarrow CS^* + OS^*$$
$$CS^* + xHS^* \rightarrow CH_xS^* + xS^*$$
$$CHxS^* + yHS^* \rightarrow CH_{x+y}S^* + yS^*$$
$$(2)\qquad C_nH_mS^* + CH_xS^* \rightarrow C_{n+1}H_{m+x}S^* + S^*.$$

The dissociation of CO needs an atomic ensemble and the chain growth requires an even greater ensemble (40, 41). Therefore, a greater crystal size favors both steps (1) and (2) to occur. There is a critical crystal size below which only CO dissociation occurs (reaction 1) yielding mainly CH_4. In addition, the olefin yield increases with the basicity of the support (12).

Although disclosing the mechanism of this reaction is beyond the aim of this work, a possible explanation coherent with the observed results, might be the following:

(a) The idea that the promoter (basic oxides) can donate electrons to the metal, increasing its electron density and favoring the reaction (1) through the backbonding of metal electrons to the antibonding orbitals of CO, weakening the C–O bond, and strengthening of C-metal bond, has been the first explanation for the promoter role and does not loose its popularity with time (4, 12, 42). However, it is possible to conclude that this theory is not physically correct (43), because not many electrons are transferred and therefore, the metal crystal cannot change its electronic density notably.

Theoretical models have demonstrated that the main effect of alkaline ions is electrostatic (44, 45), which is essentially of short range. However, a long range effect is possible as a result of a cumulative electrostatic field (45). Therefore, when a CO is adsorbed on a metal, its "O"-end interacts with the neighbor alkaline cation. Consequently, the energy of CO molecular orbitals shift downward below the Fermi level increasing the capability of the metal to donate electrons into empty orbitals of CO (44). The overall effect is that the bond between the metal and the CO becomes stronger while at the same time the intramolecular CO bond is weakened. These calculations and the experimental evidences obtained from thermal desorption spectra and vibrational spectroscopy would confirm the last explanation for the promoter effect of alkaline ions (45).

(b) A higher basicity means that less of the weakly bound, active hydrogen is available at the surface and hence hydrogenation activity is lower. This causes a decrease in the production of CH_4 and a higher content of olefins in the hydrocarbon products (12).

All the above-mentioned arguments lead to the conclusion that the selectivity to olefins of the catalysts depends on two effects: metal crystal size and basicity of the support.

c-2 shows a higher olefins/paraffins ratio than c-0 (Fig. 11), as c-2 has a crystal size similar to c-0, we consider that in this case the effect of higher basicity dominates. In c-4 there is a simultaneous increase of the crystal size and basicity, leading to a greater selectivity. For c-8 the size of crystals has fallen below the value necessary to allow reaction (2) to occur. This effect contributes to decrease the olefin selectivity. This is confirmed in Fig. 12, where it is possible to see that c-8 is the catalyst that produces more CH_4. In view of all these facts we conclude that there is a critical amount of MgO at the surface which controls the particle size and at the same time produces an optimal basicity for a good selectivity to olefins.

Figure 13 compares the total activity for hydrocarbon synthesis of c-t and c-4. It is apparent that the activity of the former on stream decreases with time faster than the latter. The activity for catalyst c-t has not reached steady-

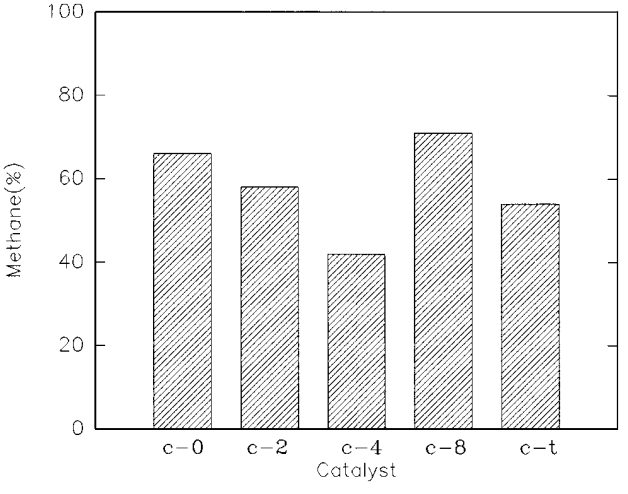

FIG. 12. Methane yield of the catalysts at steady state.

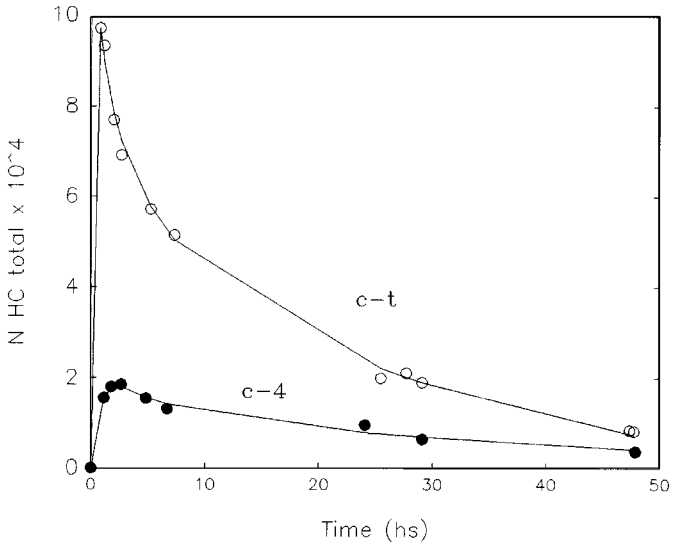

FIG. 13. Total turnover frequency vs time of reaction for c-t and c-4 catalysts.

state values even after 48 h. Besides, p-t does not show stability with storage time (we have observed some aging due to hydration and/or to carbonation). If the tendency to the deactivation of the catalysts and the aging (or lack of stability) of the precursor of c-t are considered, a clear advantage for the use of c-4 appears.

CONCLUSIONS

(1) The addition of MgO to SiO_2 support produces:

(a) the covering of the surface of SiO_2,
(b) the modification of the metallic crystal size,
(c) an increase of the activity to total hydrocarbon with the amount of MgO added.

(2) There is an optimal amount of MgO (around 4%) which produces the highest selectivity to olefins and lower CH_4 yield.

(3) The catalyst c-4 is the most attractive since it shows on stream a greater time stability and does not have disadvantages for storage, although it has a lower activity toward total hydrocarbons than c-t.

ACKNOWLEDGMENTS

The authors acknowledge support of this work by Consejo Nacional de Investigaciones Científicas y Técnicas, Comisión de Investigaciones Científicas Pcia. Bs. As. and Universidad Nacional de La Plata. Helpful discussions and encouraging comments by N. W. Delgass that improved the presentation of this paper are gratefully appreciated.

REFERENCES

1. Vannice, M. A., *J. Catal.* **37**, 449 (1975).
2. Vannice, M. A., *J. Catal.* **50**, 228 (1977).
3. Amelse, J. A., Butt, J. B., and Schwartz, L. H., *J. Phys. Chem.* **82**, 5 (1978).
4. Kellner, C. S., and Bell, A. T., *J. Catal.* **75**, 251 (1982).
5. Yung, H. J., Vannice, M. A., Mulay, L. N., Stanfield, R. M., and Delgass, W. N., *J. Catal.* **76**, 208 (1982).
6. van Dijk, W. L., Niemantsverdriet, J. W., van der Kraan, A. M., and van der Baan, H. S., *Appl. Catal.* **2**, 273 (1982).
7. Barrault, J., Forguy, C., and Perrichon, V., *Appl. Catal.* **5**, 119 (1983).
8. Yeh, E. B., Schwartz, L. H., and Butt, J. B., *J. Catal.* **91**, 241 (1985).
9. Jones, V. K., Neubauer, L. R., and Bartholomew, C. H., *J. Phys. Chem.* **90**, 4832 (1986).
10. Venter, J., Kaminsky, M., Geoffroy, G. L., and Vannice, M. A., *J. Catal.* **103**, 450 (1987).
11. Kreitman, K. M., Baerns, M., and Butt, J. B., *J. Catal.* **105**, 319 (1987).
12. Snel, R., *Catal. Rev. Sci. Eng.* **29**(4), 361 (1987).
13. Malessa, R., and Baerns, M., *Ind. Eng. Chem. Res.* **27**, 279 (1988).
14. Venter, J. J., and Vannice, M. A., *Catal. Lett.* **7**, 219 (1990).
15. Janardanaro, M., *Ind. Eng. Chem. Res.* **29**, 1735 (1990).
16. Bartholomew, C. H., New trends in CO activation, in "Studies *in* Surface Science and Catalysts" (L. Guczi, Ed.), p. 158. Elsevier, Amsterdam, 1991.
17. Cagnoli, M. V., Marchetti, S. G., Gallegos, N. G., Alvarez, A. M., Yeramián, A. A., and Mercader, R. C., *Mater. Chem. Phys.* **27**, 403 (1991).
18. Cagnoli, M. V., Marchetti, S. G., Gallegos, N. G., Alvarez, A. M., Mercader, R. C., and Yeramian, A. A., *J. Catal.* **123**, 21 (1990).
19. Boudart, M., Delbouille, A., Dumesic, J. A., Khammouma, S., and Topsøe, H., *J. Catal.* **37**, 486 (1975).
20. Marchetti, S. G., Bengoa, J. F., Cagnoli, M. V., Alvarez, A. M., Gallegos, N. G., Yeramián, A. A., and Mercader, R. C., *Meas. Sci. Technol.* **7**, to appear (1996).
21. Vandenberghe, R. E., de Bakker, P. M. A., and De Grave, E., *Hyperfine Interact.* **83**, 29 (1994).
22. Wivel, C., and Mørup, S., *J. Phys. E* **14**, 605 (1981).
23. Raupp, G. B., and Delgass, W. N., *J. Catal.* **58**, 337 (1979).
24. Kündig, W., Bommel, H., Constabaris, G., and Lindquist, R. H., *Phys. Rev.* **142**, 327 (1966).
25. Bødker, F., Mørup, S., Oxborrow, C. A., Linderoth, S., Madsen, M. B., and Niemantsverdriet, J. W., *J. Phys. Cond. Matt.* **4**, 6555 (1992).
26. Topsøe, H., Dumesic, J. A., and Mørup, S., "Applications of Mössbauer Spectroscopy" (R. L. Cohen, Ed.), Vol. 2. Academic Press, New York, 1980.
27. Marchetti, S. G., Alvarez, A. M., Mercader, R. C., and Yeramián, A. A., *Appl. Surf. Sci.* **29**, 443 (1987).
28. Mørup, S., and Topsøe, H., *Appl. Phys.* **11**, 63 (1976).
29. Boudart, M., Dumesic, J. A., and Topsøe, H., *Proc. Natl. Acad. Sci. USA* **74**, 806 (1977).
30. Niemantsverdriet, J. W., van der Kraan, A. M., Delgass, W. N., and Vannice, M. A., *J. Phys. Chem.* **89**, 67 (1985).
31. Clausen, B. S., and Topsøe, H., *Appl. Catal.* **48**, 327 (1989).
32. Travis, J. C., and Spijkerman, J. J., "Mössbauer Effect Methodology" (I. Gruverman, Ed.), Vol. 4. Plenum, New York, 1968.
33. Bianchi, D., Borcar, S., Teule-Gay, F., and Bennet, C. O., *J. Catal.* **82**, 442 (1983).
34. Topsøe, H., Topsøe, N., and Bohlbro, H., "Proceedings, 7th International Congress on Catalysts, Tokyo, 1980" (T. Seiyama and K. Tanabe, Eds.). Elsevier, Amsterdam, 1981.
35. Amelse, J. A., Schwartz, L. H., and Butt, J. B., *J. Catal.* **72**, 95 (1981).
36. Butt, J. B., "Fundamentals and Applications of Fischer-Tropsch Synthesis," AICHE Spring National Meeting, Orlando, FL, 1990.
37. Moon, S. H., Park, C. W., and Shin, H. K., "Proceedings, 10th International Congress on Catalysts, Budapest, 1992" (L. Guczi,

F. Solymosi, and P. Tetenyis, Eds.). Akadémiiai. kiadé, Budapest, 1993.
38. Rameswaran, M., and Bartholomew, C. H., *J. Catal.* **117**, 218 (1989).
39. Mc Donald, M. A., Storm, D. A., and Boudart, M., *J. Catal.* **102**, (1986).
40. Boudart, M., and Mc Donald, M. A., *J. Phys. Chem.* **88**, 2185 (1984).
41. Ponec, V., and van Barnevelt, W. A., *Ind. Eng. Chem. Prod. Res. Dev.* **18**, 4 (1979).
42. Dry, M., Shingles, T., Boshoff, L., and Vos-thuisen, A., *J. Catal.* **15**, 190 (1969).
43. Ponec, V., "New trends in CO activation," *in* "Studies in Surface Science and Catalysis" (L. Guczi, Ed.), p. 117. Elsevier, Amsterdam, 1991.
44. Bonacic-Koutecký, V., Koutecký, J., Fantucci, P., and Ponec, V., *J. Catal.* **111**, 409 (1988).
45. Niemantsverdriet, J. W., "Spectroscopy in Catalysis." VCH, Weinheim, 1993.